Electron Raman scattering in cylindrical quantum wires

1995 J. Phys.: Condens. Matter 7 7273

(http://iopscience.iop.org/0953-8984/7/36/016)

J. Phys.: Condens. Matter 7 (1995) 7273–7281. Printed in the UK

Electron Raman scattering in cylindrical quantum wires

J M Bergues†, R Riera†, F Comas‡ and C Trallero-Giner‡

† Department of Physics, University of Oriente, Santiago de Cuba, Cuba
‡ Department of Theoretical Physics, Havana University, Vedado 10400, Havana, Cuba

Received 29 December 1994, in final form 22 May 1995

Abstract. The differential cross-section (DCS) for an electron Raman scattering (ERS) process in a semiconductor quantum wire (QW) of cylindrical geometry is calculated for $T = 0$ K and neglecting phonon-assisted transitions. Electron states are considered assuming complete confinement within the QW. We also assume single parabolic conduction and valence bands. Two kinds of spectrum are discussed: emission spectra (DCS as a function of emitted photon energy) and excitation spectra (DCS as a function of incident photon energy). In both cases we analyse the DCS for different scattering configurations. We study selection rules for the processes. Singularities in the spectra are found and interpreted. The ERS studied here can be used to provide direct information about the electron band structure of the system.

1. Introduction

Raman scattering experiments are well known to provide a powerful tool for the investigation of different physical properties of semiconductor nanostructures (superlattices, quantum wells, etc) (Cardona and Güntherodt 1989, Klein 1986, Cardona 1990). In particular the electronic structure of semiconductor materials and nanostructures can be thoroughly investigated considering different polarizations for the incident and emitted radiation (Pinczuk and Burstein 1983, Cardona and Güntherodt 1989). In connection with this kind of experiment the calculation of the differential cross-section (DCS) for Raman scattering remains a rather interesting and fundamental issue to achieve a better understanding of the manufactured semiconductor nanostructures characterized by their mesoscopic dimensions (Colvard *et al* 1985, Sood *et al* 1985, Cros *et al* 1992, Shields *et al* 1992). Among the various Raman scattering processes involved in this kind of research electron Raman scattering (ERS) seems to be a useful technique providing direct information on the energy band structure and the optical properties of the investigated systems. ERS is qualitatively explained as a two-step process: in the first-step the system absorbs a photon from the incident radiation and an electron–hole pair (EHP) is created in a virtual state (after an interband electron transition); in the second step the electron and the hole move independently of each other and emit photons of secondary radiation performing intraband transitions (Riera *et al* 1988). In the final state an EHP appears in a real state of the system, which is thus left in an excited state. The DCS for ERS, in the general case, usually shows singularities related to interband and intraband transitions. This latter result strongly depends on the scattering configurations: the structure of the singularities is varied when the photon polarizations change (Cardona and Güntherodt 1982). This peculiar feature of ERS allows us to determine the subband structure of the system by direct inspection of the singularity positions in the spectra.

0953-8984/95/367273+09$19.50

For bulk semiconductors ERS has been studied in the presence of external applied magnetic and electric fields (Wallis and Mills 1970, Comas *et al* 1985, Goltzev *et al* 1979, Bechstedt *et al* 1975). In the case of a quantum well preliminary results were reported by Riera *et al* (1988). In the present article our aim is to study ERS in a quantum wire (QW) of cylindrical shape. In these novel systems the emission and excitation spectra are significantly modified due to the quasi-one-dimensional character of the electronic states. The ERS processes are determined by electronic transitions between one-dimensional electron or hole subbands. For the sake of simplicity we assume complete electron confinement within the QW. We also consider parabolic bands in the zero-temperature case and neglect all the transitions assisted by phonons. Such simplifying assumptions facilitate the calculations but still provide a clear picture of the physical situation.

2. Model and applied theory

Let us briefly describe the model and fundamental theory applied in our calculations. The QW geometry is cylindrical with circular cross-section of radius r_0. As explained above, we consider a single conduction (valence) band, which is split into a subband system due to complete electron confinement within the structure. The solution of the Schrödinger equation in the envelope function approximation leads to

$$\Psi_c = \chi_c u_c = \left[\sqrt{\pi L} r_0 J'_{n_e}(x_{n_e m_e})\right]^{-1} J_{n_e}\left(x_{n_e m_e}\frac{r}{r_0}\right)\exp(-\mathrm{i}(n_e\phi + k_e z))u_c \tag{1}$$

for conduction electrons. In equation (1) $J_n(x)$ is the Bessel function of order n. x_{nm} denotes the zeros of the Bessel function: $J_n(x_{nm}) = 0$. u_c is the Bloch function taken at $k_0 = 0$ in the Brillouin zone, where (by assumption) the band extrema are located. We use cylindrical coordinates r, θ, z. The complete electron confinement in the QW implies $\chi_c|_{r_0} = 0$.

The suffix e is used to denote electronic quantities. The electronic states are described by the quantum numbers: n_e, m_e, k_e. The eigenenergies are

$$E_c(n_e, m_e, k_e) = \frac{\hbar^2}{2\mu_e}\left[k_e^2 + \left(x_{n_e m_e}/r_0\right)^2\right] \tag{2}$$

μ_e being the electron effective mass and $E = 0$ at the bottom of the bulk conduction band. For the holes the analogous quantities are obtained essentially by replacing suffix e by h (labelling hole quantities).

The DCS for ERS is given by (Riera *et al* 1988)

$$\frac{\mathrm{d}^2\sigma}{\mathrm{d}\omega_s\,\mathrm{d}\Omega} = \frac{V^2\omega_s^2 n(\omega_s)}{8\pi^3 c^4 n(\omega_l)} W(\omega_s, \boldsymbol{e}_s) \tag{3}$$

where $V = \pi r_0^2 L$ is the normalization volume, $n(\omega)$ is the refraction index as a function of the radiation frequency, ω_s and $\boldsymbol{e}_s$ are the frequency and unit polarization vector for the emitted secondary radiation. c is the light velocity and ω_l is the frequency of the incident radiation. $W(\omega_s, \boldsymbol{e}_s)$ is the transition rate calculated according to

$$W(\omega_s, \boldsymbol{e}_s) = \frac{2\pi}{\hbar}\sum_f |M_e + M_h|^2\,\delta(E_f - E_i) \tag{4}$$

where

$$M_j = \sum_a \frac{\langle f|H_{js}|a\rangle\langle a|H_l|i\rangle}{E_i - E_a + \mathrm{i}\Gamma_a} + \sum_b \frac{\langle f|H_l|b\rangle\langle b|H_{js}|i\rangle}{E_i - E_b + \mathrm{i}\Gamma_b}. \tag{5}$$

In (5) $j = e, h$ for the cases of electrons or holes, respectively, $|i\rangle$ and $|f\rangle$ denote initial and final states of the system with their corresponding energies E_i and E_f. $|a\rangle$ and $|b\rangle$ are intermediate states with energies E_a and E_b while Γ_a and Γ_b are the corresponding lifetime broadenings.

The operator H_l is of the form

$$H_l = \frac{|e|}{\mu_0}\sqrt{\frac{2\pi\hbar}{V\omega_l}}e_l \cdot P \qquad P = -i\hbar\nabla \tag{6}$$

where μ_0 is the free electron mass. This operator describes the interaction with the incident radiation field in the dipole approximation. The interaction with the secondary radiation field is described by the operator

$$H_{js} = \frac{|e|}{\mu_j}\sqrt{\frac{2\pi\hbar}{V\omega_s}}e_s \cdot P \qquad j = e, h. \tag{7}$$

The latter operator describes the photon emission by the electron (hole) after transitions between conduction (valence) subbands of the system. In (5) the intermediate states $|a\rangle$ represent an EHP in a virtual state (after absorption of the incident photon), while the states $|b\rangle$ are related to the 'interference diagrams' (Riera *et al* 1988, Comas *et al* 1986). This latter term involves a negligible contribution whenever the energy gap E_g is large enough (for instance, this is the case for GaAs, CdTe, etc) and will not be considered in the present work.

In the initial state $|i\rangle$ we have a completely occupied valence band, unoccupied conduction band and an incident photon of energy $\hbar\omega_l$. Hence

$$E_i = \hbar\omega_l. \tag{8}$$

The final state $|f\rangle$ involves an EHP in a real state and a secondary-radiation emitted photon of energy $\hbar\omega_s$. Hence

$$E_f = \frac{\hbar^2}{2\mu_e}\left[\left(x_{n_e m_e}/r_0\right)^2 + k_e^2\right] + \frac{\hbar^2}{2\mu_h}\left[\left(x_{n_h m_h}/r_0\right)^2 + k_h^2\right] + \hbar\omega_s + E_g. \tag{9}$$

For the intermediate states $|a\rangle$ the energies E_a are easily obtained from the above discussion.

3. Differential cross-section

Using the theory depicted in section 2 we can obtain, after tedious calculations, explicit expressions for the DCS of the ERS process. In all our calculations we neglect the photon wavevector in comparison with the electron wavevector. Hence, in the final state we have $k_e + k_h = 0$. We just write the final results:

$$\left[\frac{d^2\sigma}{d\omega_s\, d\Omega}\right] = \left[\frac{d^2\sigma}{d\omega_s\, d\Omega}\right]_{e_{sz}} + \left[\frac{d^2\sigma}{d\omega_s\, d\Omega}\right]_{e_s^+} + \left[\frac{d^2\sigma}{d\omega_s\, d\Omega}\right]_{e_s^-} \tag{10}$$

where

$$\left[\frac{d^2\sigma}{d\omega_s\, d\Omega}\right]_{e_{sz}} = \frac{9\sigma_0}{2\sqrt{2}}\sum_{n_e m_e n_h m_h}\sqrt{g^2 + \sqrt{g^4 + \delta_f^4}}\,\Delta(n_e - n_h)\Delta(m_e - m_h)|e_s \cdot \hat{Z}|^2 \tag{11}$$

$$\left[\frac{\mathrm{d}^2\sigma}{\mathrm{d}\omega_s\,\mathrm{d}\Omega}\right]_{e_s^{\pm}} = \frac{9\sigma_0}{4\sqrt{2}}(\hbar\omega_s/E_0)^2 \sum_{n_e m_e n_h m_h} \left\{ \left(\frac{\beta}{1+\beta}\right)^2 \left|\frac{Y^{\mp}_{n_e m_e m_h}}{p_e + \mathrm{i}\,\delta}\right|^2 \Delta(n_h - n_e - 1) + \left(\frac{1}{1+\beta}\right)^2 \left|\frac{Y^{\mp}_{n_h m_h m_e}}{p_h + i\,\delta}\right|^2 \Delta(n_e - n_h - 1) \right\} \left[\frac{g^2 + \sqrt{g^4 + \delta_f^4}}{g^4 + \delta_f^4}\right]^{1/2} |e_s \cdot \sigma_{\pm}|^2. \tag{12}$$

We are applying the following notation for the Kronecker delta:

$$\Delta(x) = \begin{cases} 1 & x = 0 \\ 0 & x \neq 0. \end{cases} \tag{13}$$

We also have

$$\sigma_0 = \frac{4\sqrt{2}Ve^4\,|e_l \cdot p_{cv}|^2\, n(\omega_s)\mu_r^{1/2}E_0^{3/2}}{9\pi^2\mu_0^2\hbar^4c^4 n(\omega_l)\omega_l\omega_s} \tag{14}$$

and

$$\beta = \frac{\mu_h}{\mu_e} \qquad \mu_r^{-1} = \mu_e^{-1} + \mu_h^{-1} \qquad E_0 = \frac{\hbar^2}{2\mu_r r_0^2} \tag{15}$$

$$g^2 = \frac{1}{E_0}(\hbar\omega_l - \hbar\omega_s - E_g) - \frac{\mu_r}{\mu_e}x^2_{n_e m_e} - \frac{\mu_r}{\mu_h}x^2_{n_h m_h} \tag{16}$$

$$p_e = \frac{\hbar\omega_s}{E_0} + \frac{\mu_r}{\mu_e}\left(x^2_{n_e m_e} - x^2_{n_h m_h}\right) \tag{17}$$

$$p_h = \frac{\hbar\omega_s}{E_0} - \frac{\mu_r}{\mu_h}\left(x^2_{n_e m_e} - x^2_{n_h m_h}\right). \tag{18}$$

In the deduction of (10), (11) and (12) we have taken

$$\delta(E_i - E_f) \to \frac{1}{\pi}\frac{\Gamma_f}{(E_f - E_i)^2 + \Gamma_f^2} \tag{19}$$

assuming a finite lifetime for the EHP in the final state, while

$$\delta_f = \sqrt{\frac{\Gamma_f}{E_0}} \qquad \delta = \frac{\Gamma}{E_0}.$$

We also have

$$Y^{\pm}(n\,,\,l\,,\,m) = \frac{x_{n\pm1,m}x_{nl}}{x_{nl}^2 - x_{n\pm1,m}^2} \tag{20}$$

and

$$\sigma_{\pm} = \frac{1}{\sqrt{2}}\left(\hat{\boldsymbol{X}} \pm \mathrm{i}\hat{\boldsymbol{Y}}\right). \tag{21}$$

The vectors $\hat{\boldsymbol{X}}$, $\hat{\boldsymbol{Y}}$ and $\hat{\boldsymbol{Z}}$ are unit vectors along the corresponding Cartesian axes.

For the interband matrix element of operator $\boldsymbol{P}$ we use the notation

$$\boldsymbol{P}_{cv} = \frac{1}{V_0}\int_{V_0} u_c^* \boldsymbol{P} u_v\,\mathrm{d}^3r. \tag{22}$$

The above matrix element is evaluated at $\boldsymbol{k}_0 = \boldsymbol{0}$ of the Brillouin zone while V_0 is the unit cell volume.

Let us make some remarks concerning the above equations. For a general scattering configuration we should have three terms in the DCS, as explicitly seen in (10). However, for particular choices of the scattering configuration some of these terms could be absent. For instance, if we have backscattering configuration with $\hat{Z}$ parallel to the radiation wavevector $\boldsymbol{k}$, then (11) will not contribute to the DCS. In particular for the scattering configuration $\bar{Z}(e_l, \sigma_\pm)Z$ the contribution to the DCS is given by (12). In the configuration where scattered radiation wavevector is parallel to the x-axis with polarization $e_s \parallel \hat{z}$, i.e., $\bar{Z}(e_l, e_{sz})X$, only the first term on the right-hand side of equation (10) will be present in the DCS. In the $\bar{Z}(e_l, \sigma_\pm)Z$ configuration the emission spectrum of ERS in a QW shows maxima at the following values of ω_s:

$$\omega_s \to \omega_e(n_e; m_e, m_h) = \frac{\mu_r E_0}{\mu_e \hbar}\left[x^2_{n_h m_h} - x^2_{n_e m_e}\right] \tag{23}$$

$$\omega_s \to \omega_h(n_e; m_e, m_h) = \frac{\mu_r E_0}{\mu_h \hbar}\left[x^2_{n_e m_e} - x^2_{n_h m_h}\right]. \tag{24}$$

As can be seen from (23) or (24) these frequencies correspond to electron transitions connecting the subband edges for a process involving just the conduction or just the valence band (i.e., intraband transitions). The following selection rule is fulfilled: $n_e = n_h \pm 1$; the minus sign applies to (23) and the plus sign to (24).

Other singularities of (12) occur whenever $g = 0$. Such singularities are mainly related to certain values of the frequency ω_l of the incident photon. For the excitation spectra the positions of these singularities are given as follows:

$$\omega(n_e; m_e, m_h) = \frac{1}{E_0}(\hbar\omega_l - E_g) = \frac{\hbar\omega_s}{E_0} + \frac{\mu_r}{\mu_e}x^2_{n_e m_e} + \frac{\mu_r}{\mu_h}x^2_{n_h m_h}. \tag{25}$$

Here the $n_e = n_h + 1$ selection rule must be fulfilled. The peaks related to the latter singularities correspond to interband EHP transitions and their positions depend on the incident radiation frequency ω_l for both excitation and emission spectra. The singularities involved in (23) and (24) are independent of ω_l and correspond to intraband transitions. The latter singularities are present just in the emission spectra.

4. Discussion of the results

As discussed in section 3 we have computed the emission and excitation spectra of the ERS process for a given polarization e_s of the emitted radiation. The physical parameters entering our formulas were taken for the GaAs case: $E_g = 1.43$ eV; $\mu_e = 0.0665\,\mu_0$; $\mu_h = 0.45\,\mu_0$ (the heavy-hole band).

In order to construct the curves shown in the figures we used:

$$\frac{1}{V}\left[\frac{\mathrm{d}^2\sigma}{\mathrm{d}\omega_s\,\mathrm{d}\Omega}\right] \qquad \text{against } \hbar\omega_s/E_0$$

the so-called 'emission spectra', and also curves of

$$\frac{1}{V}\left[\frac{\mathrm{d}^2\sigma}{\mathrm{d}\omega_s\,\mathrm{d}\Omega}\right] \qquad \text{against } \frac{1}{E_0}(\hbar\omega_l - E_g)$$

the so-called 'excitation spectra'. The quantity $(1/V)\left[\mathrm{d}^2\sigma/\mathrm{d}\omega_s\,\mathrm{d}\Omega\right]$ is frequently called the 'scattering efficiency' (SE). In figure 1(a) the excitation spectrum is shown (SE against $(\hbar\omega_l - E_g)/E_0$) for the scattering configuration $\bar{Z}(e_l, \hat{Z})X$. In this case just the first term on the right-hand side of (10) contributes. Hence we do not have singularities. For certain

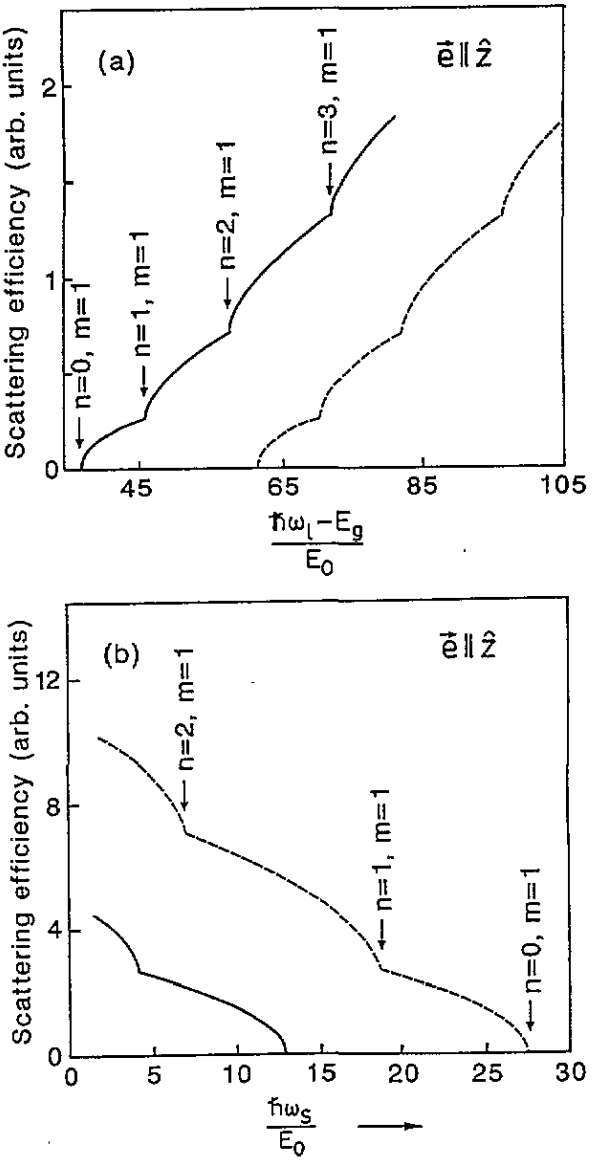

Figure 1. ERS cross-section (in arbitrary units) for a GaAs quantum wire in the scattering configuration $\bar{Z}(e_l, \hat{Z})X$. The solid curve corresponds to $r_0 = 4$ nm, the dashed curve to $r_0 = 3$ nm. We have set $\Gamma_f = 1$ meV and $\Gamma = 3$ meV. (a) scattering efficiency as a function of $(1/E_0)(\hbar\omega_l - E_g)$ (excitation spectrum). The value $\hbar\omega_s = 2.3$ eV is fixed. (b) scattering efficiency as a function of $\hbar\omega_s/E_0$ (emission spectrum). The value of $\hbar\omega_l = 2.8$ eV is fixed. The thresholds indicating different transitions between the valence and conduction subbands are labelled by (n, m) (see equation (11)).

values of ω_l we can find abrupt changes in the curve slope which correspond to different thresholds related to the points where a given subband starts to contribute to the DCS. This provides the steplike character of the curve. The lower admissible value of $\hbar\omega_l - E_g$ is defined by the minimum value of x_{nm} (i.e., x_{01}). For higher values of $\hbar\omega_l - E_g$ new subbands start to contribute, thus defining the other thresholds seen in the figure. We give

explicit indication of the points where the thresholds are present, specifying the involved subbands. In figure 1(b) the emission spectrum (SE against $\hbar\omega_S/E_0$) is shown for the same scattering configuration. The incident radiation frequency was fixed as $\hbar\omega_l = 2.8$ eV. The rest of the parameters are chosen as in figure 1(a). We again observe in the figure abrupt changes in the slope, thus providing a certain steplike dependence of the SE. The points where the curve slope presents abrupt changes are related to threshold values of $\hbar\omega_s$ again representing the incorporation of new subbands to the process. It should be realized that, for lower values of $\hbar\omega_s$, more subbands can participate in the emission process. The condition $\hbar\omega_l - \hbar\omega_s - E_g > E_0 x_{nm}^2$ must be fulfilled in order to have emission of secondary-radiation photons. For fixed values of $\hbar\omega_l$, E_g and E_0, the threshold positions are defined by x_{nm}. This is explicitly indicated in figure 1(a).

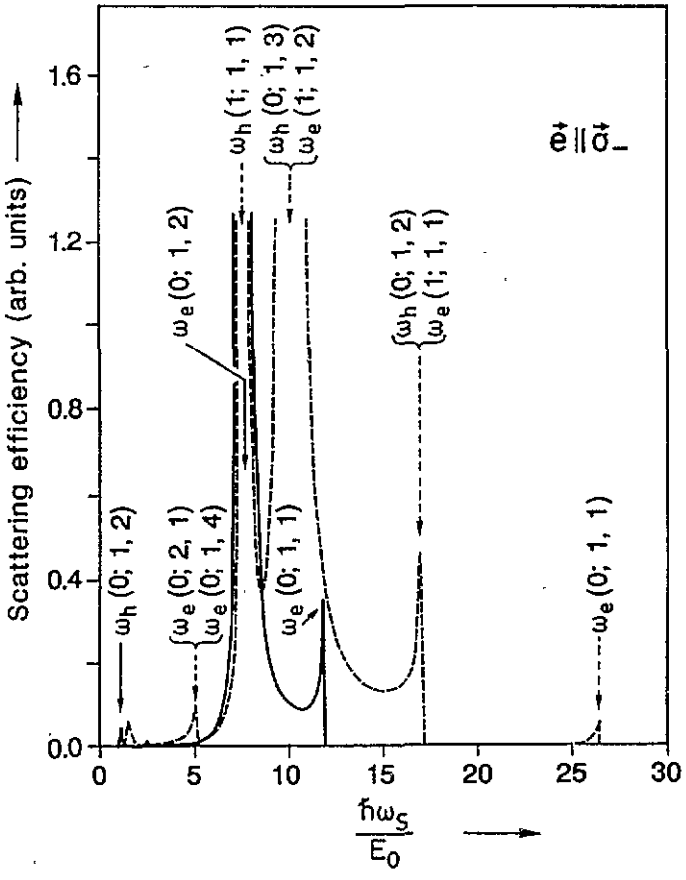

Figure 2. Scattering efficiency as a function of $\hbar\omega_S/E_0$ (emission spectrum) for a GaAs quantum wire for the $\tilde{Z}(e_l, \sigma_-)Z$ scattering configuration. The calculation was performed applying the same parameters as in figure 1. Resonant transitions are indicated by $\omega_e(n_e; m_e, m_h)$ and $\omega_h(n_e; m_e, m_h)$ corresponding to electron or hole intersubband transitions, respectively (see (23) and (24)).

In figure 2 we show the emission spectra for the $\tilde{Z}(e_l, \sigma_-)Z$ configuration. Hence, just the term with the '$-$' sign in (12) contributes. In this case we are faced with a singular behaviour of the SE; the positions of the singularities are defined by (23) and (24). We have indicated the positions of the singular points according to the notation of (23) and (24).

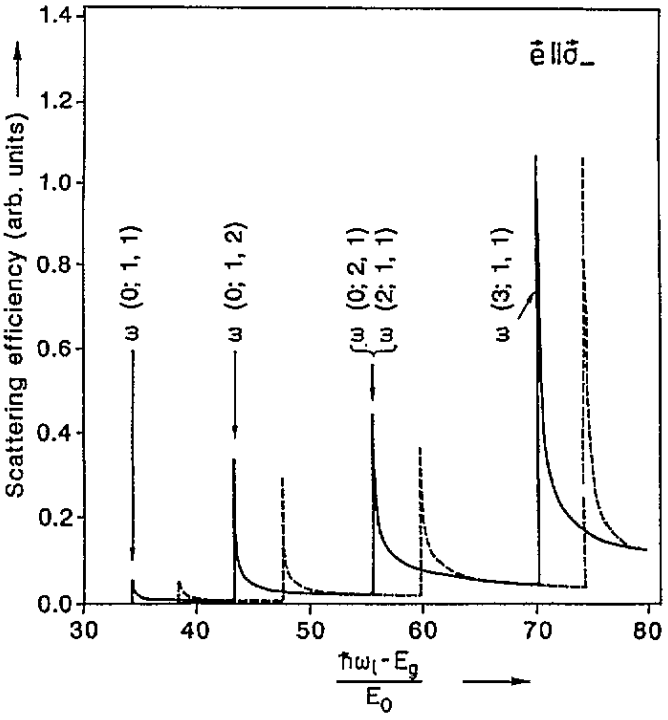

Figure 3. Scattering efficiency as a function of $(1/E_0)(\hbar\omega_l - E_g)$ (excitation spectrum) for a GaAs quantum wire in the $\bar{Z}(e_l, \sigma_-)Z$ scattering configuration. We used the same set of parameters as in figure 1. Resonant electron–hole interband transitions, following equation (25), are indicated by $\omega(n_e; m_e, m_h)$.

In figure 3 we show the excitation spectra for the same scattering configuration as in figure 2. Now $\hbar\omega_s = 2.3$ eV and $\hbar\omega_l$ is a variable quantity. The other parameters coincide with those of figure 2. We observe the singular behaviour with direct indication of the positions of the singularities. They are given by expression (25). Again we see a threshold for the lower values of $(\hbar\omega_l - E_g)E_0^{-1}$ when $x_{n_e m_e}$ and $x_{n_h m_h}$ take their minimum values.

The singular structure of the DCS, as given in the figures, provides a transparent understanding of the energy subband structure of the QW.

In the present work we have applied a simplified model for the electronic structure of the system. In a more realistic case we should consider coupled band structure using a calculation model like that of Luttinger–Kohn or the Kane model. We also assumed an infinite potential barrier for the electrons at the QW interface. A calculation assuming a finite barrier is better, but it is also possible to introduce a certain redefined effective mass for the infinite-barrier case leading to the correct energy levels for electrons and holes (see for instance Trallero-Giner and López-Gondar 1986). The mentioned assumptions would lead to better results but entail more complicated calculations. However, within the limits of our simple model we are able to account for the essential physical properties of the discussed problem. The fundamental features of the DCS, as described in our paper, should not change very much in the real QW case. It can be easily proved that the singular peaks in the DCS will be present irrespective of the model used for the subband structure and may be determined for the values of $\hbar\omega_s$ equal to the energy difference between two

subbands: $\hbar\omega_s^{e(h)} = E_\alpha^{e(h)} - E_\beta^{e(h)}$, where $E_\alpha^{e(h)} > E_\beta^{e(h)}$ are the respective electron (hole) energies in the subbands. Similarly, we will have a steplike dependence in the DCS for $\hbar\omega_l = \hbar\omega_s + E_g + E_\alpha + E_\beta$. Up to the present there is a lack of experimental work for this type of ERS. The major interest of our calculations is to stimulate experimental research in this direction.

References

Bechstedt F, Enderlein R and Peuker K 1975 *Phys. Status Solidi* b **68** 43

Cardona M 1990 *Superlatt. Microstruct.* **7** 183

Cardona M and Güntherodt G (ed) 1982 *Light Scattering in Solids II (Topics in Applied Physics 50)* (Berlin: Springer)

——1989 *Light Scattering in Solids V (Topics in Applied Physics 66)* (Heidelberg: Springer)

Comas F, Trallero Giner C, Lang I G and Pavlov S T 1985 *Fiz. Tverd. Tela* **27** 57 (Engl. Transl. *Sov. Phys.–Solid State* **27** 32)

Comas F, Trallero-Giner C and Pérez Alvarez R 1986 *J. Phys. C: Solid State Phys.* **19** 6479

Colvard C, Gant T A, Klein M V, Merlin R, Fisher R, Morkoc H and Gossard A G 1985 *Phys. Rev.* B **31** 2080

Cros A, Cantarero A, Trallero-Giner C and Cardona M 1992 *Phys. Rev.* B **46** 12 627

Goltzev A V, Lang I G and Pavlov S T 1979 *Phys. Status Solidi* b **94** 37

Klein M V 1986 *IEEE J. Quantum Electron.* **QE-22** 1760

Pinczuk A and Burstein E 1983 *Light Scattering in Solids I (Springer Topics in Applied Physics 8)* ed M Cardona (Heidelberg: Springer)

Riera R, Comas F, Trallero-Giner C and Pavlov S T 1988 *Phys. Status Solidi* b **148** 533

Shields A J, Trallero-Giner C, Cardona M, Grahn H T, Ploog K, Hoisler J A, Tenne D A, Moshegor N T and Toropov A I 1992 *Phys. Rev.* B **46** 6990

Sood A K, Menéndez J, Cardona M and Ploog K 1985 *Phys. Rev. Lett.* **54** 2111

Trallero-Giner C and López-Gondar J 1986 *Physica* B **138** 287

Wallis R F and Mills D L 1970 *Phys. Rev.* B **2** 3312